Title
An EFE model on skin-sleeve interactions during arm rotation.

Journal
Journal of biomechanical engineering, 128(6)

ISSN
0148-0731

Authors
Xing, Malcolm M Q
Sun, Zhiguo
Pan, Ning
et al.

Publication Date
2006-12-01

Peer reviewed

Malcolm M. Q. Xing

Zhiguo Sun

Ning Pan

Department of Biological System Engineering,
and Department of Chemical Engineering
and Materials Science,
University of California,
Davis, CA 95616

Wen Zhong

Department of Textile Sciences,
University of Manitoba,
Winnipeg, MB R3T 2N2, Canada

Howard I. Maibach

Department of Dermatology,
University of California,
San Francisco, CA 94143

An EFE Model on Skin-Sleeve Interactions During Arm Rotation

Skin and garment constitute a dynamic contact system for human body comfort and protection. Although dermatological injuries due to fabric actions during human body movement are common, there is still no general guidance or standard for measuring or evaluating skin/garment contact interactions, especially, during intense sports. A three-dimensional explicit finite element (EFE) model combined with Augmented Lagrange algorithm (ALA) is developed to simulate interactions between skin and fabric during rotation of the arm. Normalized effective shear stresses at the interface between skin and the sleeve during the arm rotation are provided to reflect the severity of the interactions. The effects due to changes in fabric properties, fabric-skin gap, and arm rotation rate are also illustrated. It has been demonstrated from our predictions that factors such as elastic modulus, friction coefficients, density of fabric, and the initial gap between skin and fabric influence significantly the shear stress and thus the discomfort and even injury potential to skin during intensive body movement such as sports and military. Thus this study for the first time confirms quantitatively that poorly chosen fabric with inappropriate garment design renders adverse actions on human skin. [DOI: 10.1115/1.2354205]

Keywords: skin/fabric interaction, dermatological injury, explicit finite element model (EFE), normalized Von-Mises stress, arm rotation, augmented Lagrange algorithm (ALA)

1 Introduction

Skin abrasion leads to hot spots [1]; even mild abnormality of garment/skin regulatory interaction could result in such discomfort consequences as tickling, rushing, and blistering. These irritations may turn out to be critical in athletic competition or military mission when reduced performance or mobility [2–5] becomes adversely consequential or even fatal [6]. This alone necessitates a deep investigation and understanding of interactions between garment and skin under various conditions. There have been a long string of research papers devoted to this subject. A most recent review article [7] focuses on the study and assessment methods for skin response to fabrics in static contact, in terms of changes in capillary blood flow and skin hydration. More thorough investigations on skin blisters due to friction under control conditions have been reported [8], followed by laboratory studies on the treatment of skin friction blisters [9]. Another report examined the pathophysiology, prevention, and treatment of friction-caused blisters [10]. Other studies investigated the influence of skin friction on the perception of fabric texture and pleasantness under a sequence of environmental conditions from neutral to hot-dry and hot-humid, and one conclusion is that moisture (not liquid sweet) on the skin surface increases significantly the skin friction [11]. Others analyzed the friction effects of skin in contact with five different types of materials and found that friction coefficients varied from 0.37 (skin/nylon) to 0.61 (skin/silicone) [12]. Still others applied numerical methods to simulate the friction contact effects of the soft tissues such as pigskin, and reported that stress of the specimens obtained in the case of specimens/platen friction can be greater by more than 50% than those in the case of frictionless specimens contact [13–15]. A finite element model was developed by Hendriks et al. to characterize the nonlinear mechanical responses of human skin to suctions at various pressure levels [16–18].

However, no research investigating the connections between skin abnormalities and fabric physical properties (elastic modulus, thickness, mass density, and friction coefficients), the initial gap and relative interaction intensity between skin and fabric, and have been reported, in spite of the theoretical and practical importance of the problem. So the objective of the present paper focuses on the dynamical interactions between a fabric sleeve and a rotating arm model, accounting for the above factors, by developing a robust EFE model to simulate the problem. For comparability of the numerical results, all the Von-Mises stresses are normalized into relative values.

2 Method

2.1 System Description/Analytical Model. A part of the forearm (Figs. 1(*a*) and 1(*b*)) with idealized cylindrical shape is taken as the base for simulation. For a problem like this, a two-dimensional model could not account for the fabric interactions with the skin effectively. In a 2D model, the beam or line element has to be used to represent the fabric; there are difficulties in computation for line element dynamic contact where the cross-section area of the line element is required which calls for one more dimension. The current model consists of fabric sleeve, skin, muscle, and bone so as to be closer to the actual structure. Thus a 3D model is adopted. The model consists of a fabric sleeve and skin, muscle, and bone forming the forearm. The sleeve is in a cylindrical shape but larger than the forearm, so the gap between the two enables the sleeve to drop onto the forearm due to gravity to provide the initial impact.

Also, if the model only includes the skin and fabric components and ignores the muscle and bone, it will be problematic on how to define the boundary conditions of the inner side of the skin which now interacts with the muscle. If the normal displacement of the inner skin is constrained, then the reaction force will be greater than the actual value at large angular displacement due to the unrealistic boundary constraint. The skin layer is very sensitive to the constraints due to its tiny thickness. Furthermore, the fabric interacts with skin to reduce the radial displacement because of normal constraints. If no normal constraint is assigned however, the simulation of the dynamic interaction will be difficult to continue.

The initial configuration of the model is set up like this:

Contributed by the Bioengineering Division of ASME for publication in the JOURNAL OF BIOMECHANICAL ENGINEERING. Manuscript received October 17, 2005; final manuscript received June 15, 2006. Review conducted by Jacques M. Huyghe.

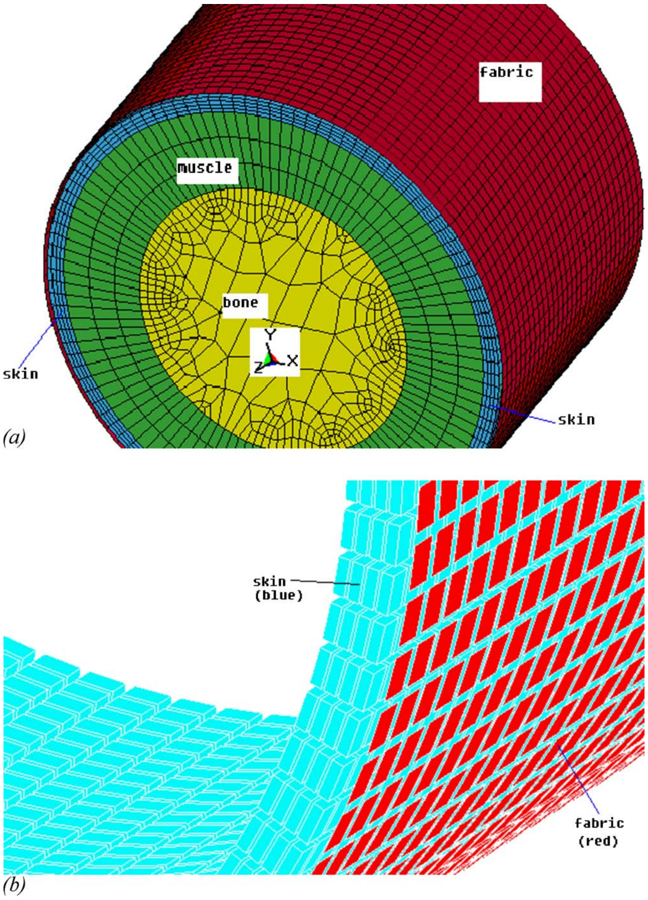

Fig. 1 ***(a)*** **Schematics of the FE model for the skin-fabric-arm system under an arm rotation. (*b*) A local view of the skin and fabric contact in the model.**

1. The arm is inside the sleeve coaxially so that there is an initial gap between the sleeve and skin.
2. Upon rotation of the arm at a given initial angular speed, the sleeve also drops freely under gravity.
3. The falling sleeve then strikes the skin on the still rotating arm.

One of the key issues in our simulation is how to deal with the contact between skin and fabric. The uncertain and more or less oscillating nature of the contact and the soft, flexible, and hyperelastic behavior of the skin presents the major difficulties in simulation. We employed the ALA, instead of the Lagrange multipliers or penalty algorithm, to cope with the problem.

So the total potential energy variation of the system during the whole dynamic interaction process can be expressed as [19,20]

$$\delta\Psi = \int_{\Gamma} [(\lambda_N + \varepsilon_N g_N)\delta g_N + (\lambda_T + \varepsilon_T g_T)\delta g_T] dA \tag{1}$$

where λ_N and λ_T are the Lagrange multipliers, ε_N and ε_T are the associated penalty parameters, and δg_N and δg_T are the virtual displacements. The subscripts N and T denote the normal and tangent directions, respectively. Also, $\lambda_T \delta g_T$ reflects the tangential sticking and the gap $g_N \geqslant 0$ assures no penetration of fabric into the skin, $\lambda_N \leqslant 0$ indicates a compressive normal stress (fabric pressure on the arm). $g_N \lambda_N = 0$ is required so that if gap is nonzero $g_N > 0$, then $\lambda_N = 0$, no contact taking place. And if the gap is zero, the contact normal force $\neq 0$.

Equation (1) can be considered as a generalization of the Lagrange multiplier method where an additional term involving the contact tractions $\lambda_T \delta g_T$ is added to the variation equation. The ALA method will alleviate the ill conditions in Penalty and Lagrange methods.

In addition to the augmented Lagrange algorithm, an automatic surface to surface contact method is used with suitable penalty parameters and stiffness factors so as to avoid the fabric from penetrating into itself at large deformation and maintaining the stability of the fabric-skin contact algorithm. The skin is considered to be the master/target and the fabric to be the slave/contact objects in the contact algorithm. In the case of fabric self-contact, however, fabric is treated as both. To ascertain skin-fabric contact state in every time step, much finer skin and fabric elements are adopted and the elements in the normal contact direction are treated with special care. All contacts in the normal direction are assumed as plane contact or the contact stresses (both tangent and normal) will approach a singular state.

Thus the global dynamic equation is

$$[K + K_c]\{u\} + [M]\{\ddot{u}\} = \{f_e\} \tag{2}$$

Here $[K]$ is the structural stiffness matrix, $[K_c]$ is contact stiffness matrix, $[M]$ is mass matrix, and $\{f_e\}$ is external force matrix (gravity); $\{u\}$ is displacement matrix and $\{\ddot{u}\}$ is acceleration matrix. The second term in the LHS accounts for the inertial force.

The boundary conditions:

for the bone: U_x, U_y, $U_z = 0$, and R_x, $R_y = 0$ (R:
rotation degree
of freedom)
for the muscle: $U_z = 0$

The initial condition:

An initial angular velocity ω_z is given for both
bone, muscle, and skin at $t = 0$

In this EFE model, the arm is represented by solid elements with skin thickness 2 mm measured by 20 MHZ ultrasound [21], whereas the fabric sleeve by shell elements with a thickness. The bending stiffness of fabric is

$$D = \frac{Eh^3}{12(1 - \nu^2)} \tag{3}$$

where E is the elastic modulus, h is the fabric thickness, and ν is Poisson's ratio [22].

Since the skin's stress-strain curve exhibits a pseudoelasticity, and hence the corresponding strain energy [23]. In our model, a time independent, isotropic, and hyperelastic constitutive model is used for skin according to Fung [22] and Gambarotta et al. [24], and the Mooney–Rivlin two-parameter constitutive equation [17,25] were employed with two-parameter C_{10} and C_{11} to present the hyperelastic properties of the skin. The bone is considered to be a rigid body, since the elastic modulus of the bone is much larger than that of the muscle or skin. Since our focus is on the interaction between skin and fabric in a very short time, the *muscle* under the skin is supposed to be elastic.

2.2 Numerical Resolution/ Software. Four numerical simulations, a, b, c, and d, under different conditions are performed to investigate the interactions between skin and fabric as the forearm is turning by some degrees in one or alternating directions during a given period of time. Each simulation examines the influence of one parameter at four different levels as detailed in Table 1. During calculation, the skin surface nodes experiencing maximum Von-Mises shear stress is located and recorded, based on the hypothesis that a higher maximum stress is more likely to cause greater skin irritation. For comparability among different simulation results, normalization is then performed by dividing all other stress values with the corresponding maximum stress in each run,

Table 1 Parameters/ranges for four simulations

Variables		Fabric modulus (MPa)	Fabric-skin uniform initial gap (mm)	Fabric-skin friction	Fabric density (10^{-4} g/mm^3)	Forearm rotation Range (radius)	Total time (s)	Speed (rad/s)
Simulation	*a*	200, 400, 600, 800	2.0	0.3	6.0	$0-\pi/2$	0–0.1	15.7
						$\pi/2-\pi/2$	0.1–0.2	31.4
	b	400	1.0	0.0,0.2,0.3,0.5	3.0	$0-\pi/2$	0–0.1	15.7
						$\pi/2-\pi/2$	0.1–0.2	31.4
	c	600	0.8, 3, 6, 8	0.3	5.0	$0-\pi/2$	0.12	13.1
	d	500	7.0	0.4	2.0, 4.0, 6.0, 8.0	$0-\pi/2$	0.12	13.1

and the normalized relative stresses are plotted against time to illustrate the interactions between the skin and the fabric sleeve during the process. The EFE analyses are performed using commercial finite element software (preprocessor: ANSYS V.6.1, explicit solver: DYNA3D, postprocessor: PostGL).

2.3 Model Parameter. Ranges of the parameters for each simulation are listed in Table 1.

It is noted that for simulations *a* and *b*, the arm rotation around axis Z (arm central rotation axis as shown in Fig. 1(*a*)) in alternating directions; from 0 to 0.1 s, the arm rotates in one direction for an angular displacement of $\pi/2$, i.e., at a constant angular velocity of 15.7 rad/s; then from 0.1 to 0.2 s, the arm reverses in opposite direction from $\pi/2$ to $-\pi/2$. In other words, the angular speed doubled to 31.4 rad/s upon reversing the rotation direction. This is different from simulations *c* and *d*, where the arm turns from 0 to $\pi/2$ in 0.12 s in one direction only.

The two-hyperelastic material properties of the skin are taken from Ref. [17] as $C_{10}=10$ kPa and $C_{11}=100$ kPa, input into the card of DYNA3D. For muscle, the normal modulus E_n is 1 MPa and tangential modulus E_t 5 kPa adopted from Ref. [26]. Thus, computational time is drastically reduced without too much compromise in accuracy. In addition, the contact relationship between parts is classified as perfect bonding (bone/muscle, muscle/skin), and dynamic sliding with friction (skin/fabric), respectively.

Since material properties of biological system tissues usually vary greatly from experimental conditions and samples, in order to test the significance of the results to evaluate their dependence on the under model parameter, we take a second set of skin parameter $C_{10}=7.1$ kPa and $C_{11}=34$ kPa [16] to simulate the effects of elastic modulus and frictional coefficients on fabric. The results are shown in Tables 2 and 3.

3 Results

In order to evaluate the shear stress or friction force, the maxima Von-Mises stress (effective shear stress) is used to characterize the skin-fabric interactions in these numerical simulations. The Von-Mises stress is defined as a function of deviated principal stress

$$\sigma_e=[(\sigma_1-\sigma_2)^2+(\sigma_2-\sigma_3)^2+(\sigma_3-\sigma_1)^2]^{\frac{1}{2}} \tag{4a}$$

or

$$\sigma_e=[(\sigma_x-\sigma_y)^2+(\sigma_y-\sigma_z)^2+(\sigma_z-\sigma_x)^2+6(\sigma_{xy}{}^2+\sigma_{zy}{}^2+\sigma_{xz}{}^2)]^{1/2} \tag{4b}$$

where σ_i is the ith principal stress, σ_j are the normal stresses at $j=x,y,z$ axes, and $\sigma_{xy,zy,xz}$ are the corresponding shear stresses, respectively.

With the hypothesis that the largest stresses contribute most significantly to skin discomfort, in our simulations we focus on the contact points suffering maximum stresses during arm rotation. In other words, in the following plots, we only provide the time when, not where, the maximum stress occurs on the skin at different levels of the related parameters.

Figure 2 shows the results for simulation *a*, where the normalized maximum effective shear stress at the skin-fabric contact interface is plotted as a function of time at four different fabric elastic modulus levels ((A) 200, (B) 400, (C) 600, and (D) 800 MPa). It is clear that in this case, all the fabric sleeves strike the arm at the same time as indicated by the peaks at around $t=0.04$ s, and the second group of peaks occur at the time the rotation direction reverses. Fabric elastic modulus exerts significant influence on the shear response of the skin, and the doubling of the rotation speed at the second period clearly impacted the shear stresses.

To examine the effects of the fabric/skin friction coefficients on the results, four different fabric/skin friction coefficients are used, respectively for simulation *b* and the normalized effective shear stresses are plotted against time in Fig. 3. Once again, the differences between the two periods of different angular speeds are apparent.

For Fig. 3, some curves are shown in more zig-zag formats; this is because during the simulation, we selected a changing sampling frequency depending on the complexities of each case. When plotting, however, we used the same number of data points so as to facilitate comparison among the curves. In other words, some curves are smoother because fewer points were used.

Results in Fig. 3 show a significant impact of the fabric friction coefficients on the skin/fabric interactions. The maximum shear

Table 2 Relative maximum Von-Mises stress with the second set skin parameters under varying fabric elastic modulus at the arm reversing point around $t=0.1$ s

Elastic modulus (MPa)	200	400	600	800
Stress peak (Normalized)	0.61	0.67	0.75	1

Table 3 Normalized maximum Von-Mises stress with the second set of skin parameters under varying frictional coefficients at arm reversing point around $t=0.1$ s

Elastic modulus (MPa)	200	400	600	800
Stress peak (Normalized)	0.46	0.73	0.81	1

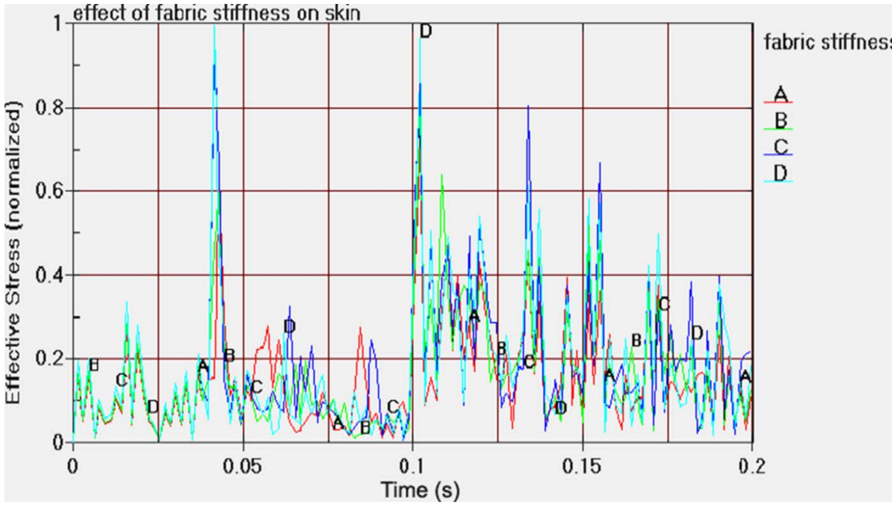

Fig. 2 Normalized effective shear stress as a function of time at four different fabric modulus levels for simulation *a*: (A) 200, (B) 400, (C) 600, and (D) 800 MPa

stress corresponds to the value of the friction coefficients, except the anomalous peak *C* with friction coefficient 0.2 at near 0.025 s for which more specific explanation is provided in Sec. 4.

Effects of initial gap between the fabric and skin are depicted in Fig. 4 at four initial gaps: 0.8 (A), 3 (B), 6 (C), and 8 mm (D). The four first-strike peaks take place according to their corresponding initial gaps, yet with samples C and D reversing the sequence. It shows that the maximum Von-Mises shear stresses are significantly greater in the case with initial gaps of 0.8 and 8 mm than those with a gap of 3 and 6 mm, respectively.

Note that curve A with initial gaps of 0.8 mm in Fig. 4 shows more peaks than other curves. This is not resulted from the numerical instability. For explicit computation, when the lost energy is smaller than 5% of the initial energy, the result is considered stable. In our simulation, the ratio of final energy to initial energy is close to 1.0. Actually, if we notice that the initial gap in this

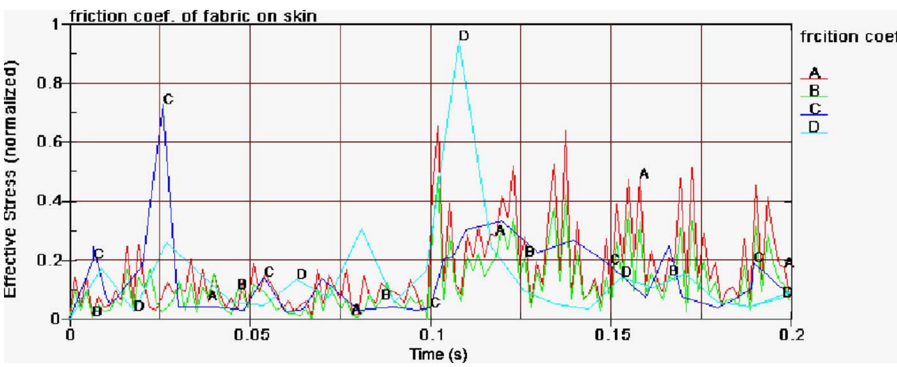

Fig. 3 Normalized effective stresses at different friction coefficients as a function of time for simulation *b*: (A) 0.3, (B) 0, (C) 0.2, and (D) 0.5

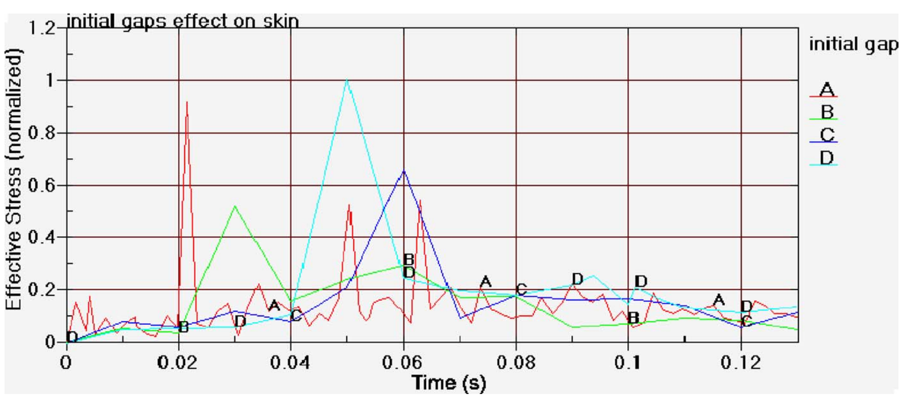

Fig. 4 Predicted effective shear stresses at different initial gap between fabric and skin as a function of the rotating time for simulation *c*. (A) 0.8, (B) 3, (C) 6, and (D) 8 mm.

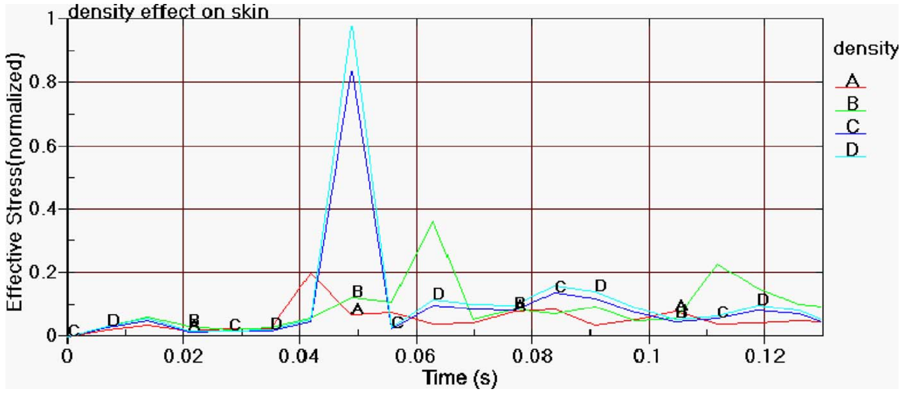

Fig. 5 Predicated normalized stress response with different fabric density as a function of rotation time for simulation *d*: (A) 2×10^{-4}, (B) 4×10^{-4}, (C) 6×10^{-4}, and (D) 8×10^{-4} g/mm^3

case is the smallest, 0.8 mm, this tighter arrangement between the skin and sleeve likely leads to more frequent interactions, thus more peaks.

The influences of the fabric density are computed as seen in Fig. 5, where, when the arm is given a constant angular velocity of 13.1 rad/s, the stress magnitude in general increases with an increasing fabric density. The first-strike peaks are supposed to locate at the same time; the peaks for samples A and B, however, occurred earlier or later.

Figure 6 shows that fabric B with a lower elastic modulus making a closer contact with the rotating arm exhibits a larger displacement due to more pliable shape conformity.

In order to further validate the simulation results, we adopt the second set of skin mechanical parameters C_{10}=7.1 kPa and C_{11}=34 kPa [16] to confirm the effects of both fabric elastic modulus and friction coefficients on the peak Von-Mises stress, and the predictions are tabulated in Tables 2 and 3. We found again pronounced peak stresses around the time t=0.1 s, the point when the arm is reversing the turning direction and thus generating excessive angular acceleration, a result similar to what was observed in the predictions using the first set of skin parameters before.

4 Discussion and Conclusions

First, as mentioned before, during each simulation, we scanned all the nodes of the fabric-skin contacts to identify the maximum stress to plot against time. Therefore, we only examined *when* and *how much*, but not *where*, a maximum stress takes place.

Next, this arm rotating is a circular motion. For the fabric sleeve to follow this circular motion, we have included a centripetal force distributed over the fabric in the model, pushing it toward the center of the circular path. The magnitude of the centripetal force is equal to the mass m of the fabric times its velocity squared v^2 divided by the radius r of its path: $F=mv^2/r$. Obviously this force plays an important role during the fabric-skin interactions.

The effects of fabric tensile modulus studied in simulation *a* are plotted in Fig. 2, which is shown to have exerted a significant influence on the shear (frictional) response of the skin.

There are two major peaks locations. The first is located at $t \approx 0.04$ s, which is most likely the point where the fabrics first strike the skin. Obviously, a stiffer fabric would generate a greater impact stress. However, the exact first strike time cannot be readily estimated by Newton's Law alone by considering fabric free falling from the height of a given initial gap, as the deformation of fabrics and fabric self-interaction may affect the first strike time. Nonetheless, this fabric-skin first strike time is clearly important and will be discussed again in other simulations below.

After the first strike, from t =0.05 to 0.1 s, it is the least stiff fabric A that generates the highest shear stress, as for a given

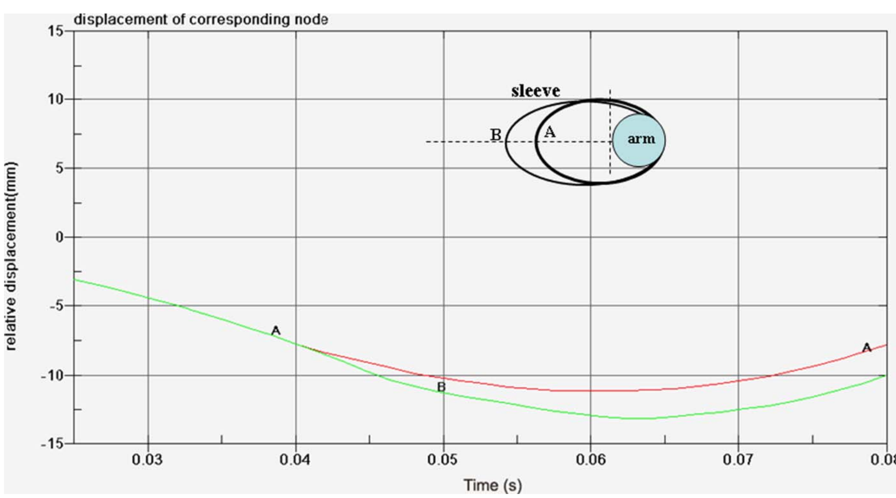

Fig. 6 Displacements of the sleeves away from the arm contacting point as a function of time at different levels of fabric elastic modulus: (A) elastic modulus: 800 MPa and (B) elastic modulus: 200 MPa

centripetal force, a less stiff fabric in general maintains a better or tighter contact with the skin during a stable circular motion, hence, the greater frictional force.

Another interesting point is at $t \geqslant 0.1$ s, when reversed arm rotation starts; the higher acceleration and greater centripetal force intensify the fabric skin impact and the peak frictional forces for all the four samples as mentioned before. It reveals that fabric/skin interactions are often of great dynamic or bumpy nature as illustrated in Fig. 2(*b*), rather than just smooth or static friction.

These characteristics are also indicated in Fig. 3, where different friction coefficients are adopted. Generally speaking, when friction coefficient is smaller, the corresponding shear stress will be the lower. However, the higher acceleration and greater centripetal force in the reverse period again cause greater skin/fabric interactions for all the samples in Fig. 3. There are possible reasons to consider the unusually high peak C with friction coefficient 0.2 at 0.025 s as anomalous; the potential fabric local folding and wrinkling at the fabric/skin interface likely result in penalty force and singular stress effect at fabric element edge.

In the following simulations *c* and *d*, a constant angular speed $\omega = 13.1$ rad/s is chosen. Effects of the initial gap between fabric and skin are studied in simulation *c* as shown in Fig. 4. It is comforting to see that samples A, B, and C strike the skin at different times according to their respective gaps, namely, the smaller the gap, the earlier the first strike. The deviation of sample D, however, again highlights the complexity of the whole process. In terms of the magnitude of impact, although a fabric with larger initial gap, and thus higher impact speed, will generate larger effective stress on the skin, it is yet to be further examined why the very close initial gap (0.8 mm) also leads to a significant peak of effective stress on the contact surface. This may suggest that when a garment is excessively tight or loose, greater shear stresses could be generated at the skin/fabric contact interface. It still needs more points to verify this suggestion. If excluding the peaks corresponding to different initial gaps in the first time period (0–0.6 s), the rest of the four curves are quite similar to each other, a consequence of the same fabrics moving at the constant angular speed 13.1 rad/s. Another possible reason may be due to the low impact speed on the skin; the fabric would have a tighter contact on the skin and a greater static friction might have contributed to an increased skin surface stress. However, once fabrics settle down, they all show quite smooth interactions with the skin, in contrast with simulations *a* and *b* where reversed arm rotation indeed complicates the situation.

Fabric density also exhibits considerable influences on the results as examined in simulation *d* with Fig. 5. Since the skin surface node with maximum effective stress is our focus in the simulation, variations of the first peak time for samples A and B are reasonable because the initial location for this node may be different for each test. Magnitudes of initial impact on the skin are just proportional to their mass as Newton would dictate. The rest of the process is a relatively smooth ride for all samples.

With the hypothesis that the largest stresses contribute most significantly to skin discomfort, in our simulations we focus on the contact points suffering maximum stresses during arm rotating and in alternating directions. It is clear from the results that increase of fabric elastic modulus, friction coefficient, initial gap, and fabric density will all enforce the skin stress. Our results should provide guidance for analyzing the skin discomfort caused by fabrics. However, the complexity and random nature of the skin-fabric interactions also generate deviations from the above predicted trends in a few cases including the time of the first stress peak, the fluctuation of stresses during the arm rotating, and the singular stress state at the boundary.

In fact, a simple analysis below can explain some of the abnormalities. For simplicity without losing generality, the skin/fabric contact model is reduced into 2D case as shown in Fig. 7. Also assumed are that the initial local contact area is very small and for

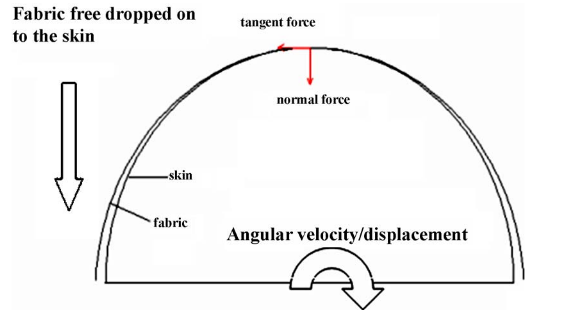

Fig. 7 Initial contact between fabric and skin with a velocity

a very short time. Thus the rotation angular displacement of the skin could be neglected. Applying Coulomb's friction law, shear traction can be determined from Ref. [27] as

$$T_x = 2\mu F_{\text{normal}}\sqrt{a^2 - x^2}/(\pi a^2) \tag{5}$$

Expand Eq. (5) at zero respective to $(x/a)^2$ leads to

$$T_x \approx 2\mu F_{\text{normal}} 1/\pi a\left[1 - 1/2\left(\frac{x}{a}\right)^2\right] \tag{6}$$

where T_x is the tangent force along the local contact area, μ is the friction coefficient, F_{normal} is the local normal force of contact, a is the approximate length of contact area, and x is the distance from the center to the edge of the contact area, and $-a < x < a$.

Our simulation results also indicate that at initial contact stage the curvature radius of the fabric with a smaller elastic modulus is lower than that of the fabric with a larger elastic modulus, so that the initial contact length a with smaller modulus will be longer than that in the case of larger modulus, and the tangent force gives the relationship $T_{x\text{largestif}} \geqslant T_{x\text{smallstif}}$, as has been shown in the simulation results of Figs. 2 and 6.

Finally, we have employed a second set of skin properties to check the influences of both fabric elastic modulus and frictional coefficients. The results shown in Tables 2 and 3 are consistent with those corresponding to the first set of skin parameters.

Simulation in this paper focuses on the arm rotation, a movement more than frequently performed in our daily life. Analysis of the model has for the first time revealed how variations of such related factors as the elastic modulus, friction coefficients, and density of the fabric, and initial gap between skin and fabric are contributing to the frictional stresses and presumably the discomfort levels of skin against cloth during our movement.

Obviously, this report only represents our initial attempt in tackling an extremely complex phenomenon. Our model just simulated a 0.2 s transient process. Time consumption was one consideration (each calculation takes about 15 h on a computer with duel CPUs and 2 GB memory). Also, it is widely believed that transient process is critical in studying human sensations. It is expected that a simulation with longer period and an integral parameter besides instantaneous values will surely provide additional information.

Furthermore, different models have been proposed to describe the skin behavior, including instance isotropic viscoelastic and hyperelastic theories [22,24], as well as the more realistic porelastic model proposed by Wu et al. [14,15].

Finally, we will conduct some experiments correspondingly to validate so as to improve the numerical model, select more appropriate material properties and constitutive equation. We will also deal with the fabric edge singular stress and the fabric contact penetration problem. In the end, we will work with interested companies to simulate the dynamic interactions between sports garment and the entire human body [28,29].

References

[1] Bruce, C. M., 2000, "The Role of Topical Lubrication in the Prevention of Skin Friction in Physically Challenged Athletes," J. Sports Chiropr. Rehab., **14**(2), pp. 37–41.

[2] Sulzberger, M. B., Cortese, T. A., Fishman, L., and Wiley, H. S., 1966, "Studies on Blisters Produced by Friction. I. Results of Linear Rubbing and Twisting Technics," J. Invest. Dermatol., **47**(5), pp. 456–465.

[3] Reynolds, K. L., White, J. S., Knapik, J. J., Witt, C. E., and Amoroso, P. J., 1999, "Injuries and Risk Factors in a 100-Mile (161-km) Infantry Road March," Prev. Med., **28**(2), pp. 167–173.

[4] Reynolds, K., Williams, J., Miller, C., Mathis, A., and Dettori, J., 2000, "Injuries and Risk Factors in an 18-Day Marine Winter Mountain Training Exercise," Mil. Med., **165**(12), pp. 905–910.

[5] Mailler, E. A., and Adams, B. B., 2004, "The Wear and Tear of 26.2: Dermatological Injuries Reported on Marathon Day," Br. J. Sports Med., **38**(4), pp. 498–501.

[6] Akers, W. A., and Sulzberger, M. B., 1972, "The Friction Blister," Mil. Med., **137**(1), pp. 1–7.

[7] Zhong, W., Xing, M., Pan, N., and Maibach, H. I., 2006, "Textiles and Human Skin, Microclimate, Cutaneous Reactions: Overview," J. Toxicol.: Cutan. Ocul. Toxicol., **25**, pp. 23–39.

[8] Naylar, P. F. D., 1955, "Experimental Friction Blisters," Br. J. Dermatol., **67**, pp. 327–342.

[9] Cortese, T. A., Jr, Fukuyama, K., Epstein, W., and Sulzberger, M. B., 1968, "Treatment of Friction Blisters—An Experimental Study," Arch. Dermatol., **97**(6), pp. 717–721.

[10] Knapik, J. J., Reynolds, K. L., Duplantis, K. L., and Jones, B. H., 1995, "Friction Blisters—Pathophysiology, Prevention and Treatment," Sports Med., **20**, pp. 136–147.

[11] Gwosdow, A. R., Stevens, J. C., Berglund, L. G., and Stolwijk, J. A. J., 1986, "Skin Friction and Fabric Sensations in Neutral and Warm Environments," Text. Res. J., **56**, pp. 574–580.

[12] Zhang, M., and Mak, A. F., 1999, "In Vivo Friction Properties of Human Skin," Prosthet. Orthot Int., **23**, pp. 135–141.

[13] Wu, J. Z., Dong, R. G., and Schopper, A. W., 2004, "Analysis of Effects of Friction on the Deformation Behavior of Soft Tissues in Unconfined Compression Tests," J. Biomech., **37**, pp. 147–155.

[14] Wu, J. Z., Dong, R. G., Smutz, W. P., and Schopper, A. W., 2003a, "Nonlinear and Viscoelastic Characteristics of Skin Under Compression: Experiment and Analysis," Biomed. Mater. Eng., **13**, pp. 373–385.

[15] Wu, J. Z., Dong, R. G., Schopper, A. W., and Smutz, W. P., 2003b, "Analysis of Skin Deformation Profiles During Sinusoidal Vibration of Fingerpad," Ann. Biomed. Eng., **31**, pp. 867–878.

[16] Hendriks, F. M., Brokken, D., van Eemeren, J., Oomens, C. W. J., Baaijens, F. P. T., and Horsten, J., 2003, "A Numerical-Experimental Method to Characterize the Non-Linear Mechanical Behaviour of Human Skin," Skin Res. Technol., **9**, pp. 274–283.

[17] Hendriks, F. M., Brokken, D., Oomens, C. W. J., and Baaijens, F. P. T., 2004, "Influence of Hydration and Experimental Length Scale on the Mechanical Response of Human Skin In Vivo, Using Optical Coherence Tomography," Skin Res. Technol., **10**, pp. 231–241.

[18] Xing, M., Pan, N., Zhong, W., and Maibach, H. I., 2006, "Skin Friction Blistering: Computer Model," Skin Res. Technol., **12**, pp. 1–7.

[19] Wriggers, P., and Zavarise, G., 1993, "Application of Augmented Lagrangian Techniques for Nonlinear Constitutive Laws in Contact Interfaces," Commun. Numer. Methods Eng., **9**, pp. 815–824.

[20] Zavarise, G., Wriggers, P., and Schrefler, B. A., 1995, "On Augmented Lagrangian Algorithms for Thermomechanical Contact Problems With Friction," Int. J. Numer. Methods Eng., **38**, pp. 2929–2949.

[21] Black, M. M., 1969, "A Modified Radiographic Method for Measuring Skin Thickness," Br. J. Dermatol., **81**, pp. 661–666.

[22] Fung, Y. C., 1984, *Biomechanics—Mechanical Properties of Living Tissues*, Springer, New York, pp. 300–304.

[23] Tong, P., and Fung, Y. C., 1976, "The Stress-Strain Relationships for the Skin," J. Biomech., **9**, pp. 649–657.

[24] Gambarotta, L., Massabo, R., Morbiducci, R., Raposio, E., and Santi, P., 2005, "In Vivo Experimental Testing and Model Identification of Human Scalp Skin," J. Biomech., **38**(11), pp. 2237–2247.

[25] Agache, P., and Humbert, P., 2004, *Measuring the Skin*, Springer-Verlag, Berlin.

[26] Blemker, S. S., Pinsky, P. M., and Delp, S. L., 2005. "A 3D model of Muscle Reveals the Causes of Nonuniform Strains in the Biceps Brachii," J. Biomech., **38**, pp. 657–665.

[27] Jager, J., 1997, "Half-Planes Without Coupling Under Contact Loading," Arch. Appl. Mech., **67**, pp. 247–259.

[28] Kenins, P., 1994, "Influence of Fiber-Type and Moisture on Measured Fabric-to-Skin Friction," Text. Res. J., **64**, pp. 722–728.

[29] Ridge, M. D., and Wright, V., 1966, "Mechanical Properties of Skin: A Bioengineering Study of Skin Structure," J. Appl. Physiol., **21**, pp. 1602–1606.